

## EXPERIMENTAL STUDY OF THE LIQUID-GLASS TRANSITION IN AN INORGANIC POLYMER $\text{Li}_{0.5}\text{Na}_{0.5}\text{PO}_3$

B. RUFFLÉ\*, S. BEAUFILS\*, Y. DÉLUGEARD\*, G. CODDENS\*\*, J. ETRILLARD\*,  
B. TOUDIC\*, M. BERTAULT\*, J. EVEN\*, J. GALLIER\*, C. ÉCOLIVET\*

\*G.M.C.M., URA CNRS 804, Université de Rennes 1, 35042 Rennes Cedex, France

\*\*Laboratoire Léon Brillouin, CE Saclay, 91191 Gif Sur Yvette Cedex, France

### ABSTRACT

New experimental results obtained with various techniques on a less-studied glass-forming system are presented. At low frequency, a secondary  $\beta_{\text{slow}}$ -process, decoupled from the viscous flow, is observed by  $^{31}\text{P}$  NMR. Raman scattering spectra and coherent neutron scattering spectra has been obtained in wide frequency and temperature ranges showing the same qualitative features for the Boson peak while the quasielastic contribution seems to differ markedly.

### INTRODUCTION

Recently, the discussion concerning the microscopic origin of the glass transition has been stimulated by the application of the mode-coupling formalism (MCT). In its idealized form, this theory predicts a dynamical phase transition from an ergodic to a non ergodic behavior at a critical temperature  $T_c$ , located above the calorimetric glass transition temperature  $T_g$ , where non-linear interactions, which become stronger with decreasing temperatures, induce a structural relaxation arrest. The mode coupling theory predicts that anomalies occur at  $T_c$  for all variables that couple to density fluctuations. Between the microscopic time scale and the structural relaxation  $\alpha$ -process, a secondary relaxation, the  $\beta_{\text{fast}}$ -process, is always observed by neutron and light scattering. Both processes are expected to exhibit scaling laws with diverging time scales at  $T_c$  [1].

Mode coupling theory has obtained some success on glass-forming systems that are classified as fragile liquids in Angell's classification [2]. So it is an open question how far this behavior depends on the degree of fragility of the system under study. However, as the spectra of these less fragile systems are characterized by a stronger vibrational contribution, the so-called Boson peak, a complete description of the dynamical structure factor  $S(q, \omega)$  should include this inelastic feature.

### MATERIAL AND METHODS

In this framework, we are studying the dynamical behavior of an alkali phosphate glass.  $\text{Na}_{0.5}\text{Li}_{0.5}\text{PO}_3$  is an inorganic polymer based on the phosphorus oxygen backbone. The basic structural unit is the  $\text{PO}_4$  group linked with two neighboring tetrahedra forming, for this alkali concentration, an infinite twisted chain. Due to the eutectic composition, the melting temperature  $T_m$  is lowered to 749 K and the calorimetric glass transition temperature  $T_g$  to 515 K.

It is well known that in order to understand the complex dynamical processes which take place at the liquid-glass transition, several different techniques must be used trying to cover the widest frequency range as possible so  $\text{Na}_{0.5}\text{Li}_{0.5}\text{PO}_3$  is studied by means of mechanical, calorimetric and dielectric spectroscopies and also by nuclear magnetic resonance [3], light and neutron scattering.

### EXPERIMENTAL RESULTS

#### Bulk properties

First, the temperature dependence of the specific heat  $C_p$  has been measured in this phosphate glass by conventional differential scanning calorimetry (Perkin-Elmer DSC7, heating rate 10 K/min) leading to a calorimetric glass transition temperature  $T_g$  of 515 K as shown in Fig. 1. It is interesting to note the relative magnitude of  $\Delta C_p/C_p$  which is often proposed as an indication of the fragility of the liquid. In the case of this phosphate glass, it amounts to 40% like in ortho-terphenyl, one of the most fragile liquids.

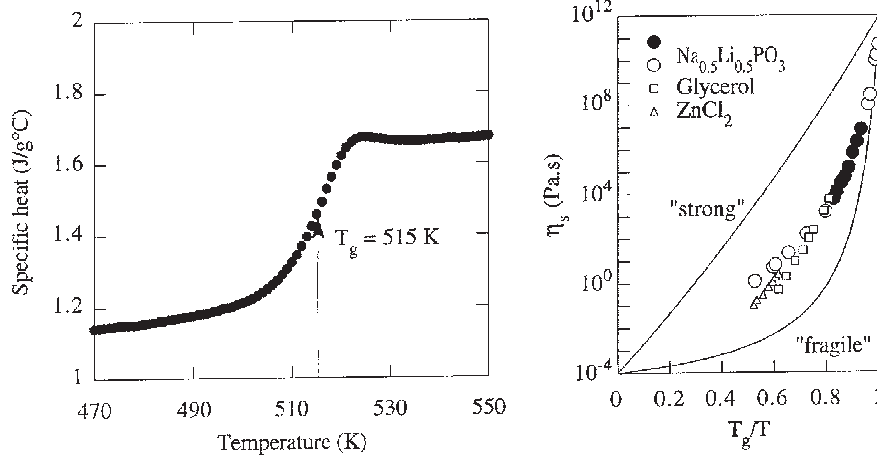


Fig. 1. (left) Temperature dependence of the specific heat in  $\text{Na}_{0.5}\text{Li}_{0.5}\text{PO}_3$  leading to  $T_g=515\text{K}$  with a relative jump  $\Delta C_p/C_p$  of about 40%

Fig. 2. (right) Temperature dependence of the viscosity for  $\text{Na}_{0.5}\text{Li}_{0.5}\text{PO}_3$  (○ from [4,5], ● from [6]) as compared to glycerol (□) and  $\text{ZnCl}_2$  (Δ) from [1].

In order to better characterize the temperature dependence of the structural process, shear viscosity data have been obtained in an intermediate temperature range between those near  $T_g$  [4] and those around  $T_m$  [5]. As shown in Fig. 2, this eutectic composition occupies an interesting position among known glass-forming systems between strong and fragile liquid just as two others, glycerol and  $\text{ZnCl}_2$ . However, the strong apparent activation energy of the viscosity at  $T_g$  leads to a fragility parameter

$$m = \left. \frac{d \log(\eta_s)}{d(T_g/T)} \right|_{T=T_g} = 79. \quad (1)$$

Again, this value is very close to  $m=81$  found in ortho-terphenyl [7].

#### Low frequency dynamics

Applying  $^{31}\text{P}$  and  $^7\text{Li}$  NMR on this phosphate glass [3], it has been shown that below  $T_g$ , the NMR parameters are mainly determined by the lithium diffusion in the amorphous structure. This motion seems unaffected by the glass transition and its spectral density is linearly frequency dependent in the two probed frequency ranges (MHz and KHz). Above  $T_g$ , the  $\text{PO}_4$  units of the phosphate chains move isotropically, giving rise to the so-called secondary relaxation in glasses ( $\beta_{\text{slow}}$ -process) while the primary or structural relaxation ( $\alpha$ -process) is only effective on the NMR parameters near 600 K, well above  $T_g$ . In Fig. 3 are plotted the relaxation time of this  $\beta_{\text{slow}}$ -process deduced from the NMR study and the timescale  $\tau_s$  of the structural relaxation simply calculated with the Maxwell relation ( $\tau_s = \eta_s / G_\infty$ ). It seems that below 600 K, the time scales of these two processes are strongly decoupled, giving rise to a primary slow relaxation and to a secondary one. Such motion decoupling has been recently reported on another phosphate glass [8]

(*m*-tricesyl phosphate) at the critical temperature  $T_c$  of the MCT determined by scaling laws analysis of the light scattering susceptibilities. Well under  $T_g$ , the relaxation times measured by Dynamical Mechanical Analysis (DMA) [9] in  $\text{Na}_{0.5}\text{Li}_{0.5}\text{PO}_3$  are also shown in Fig. 3. Obviously, the same secondary relaxation is probed in these macroscopic measurements of the dynamical Young modulus.

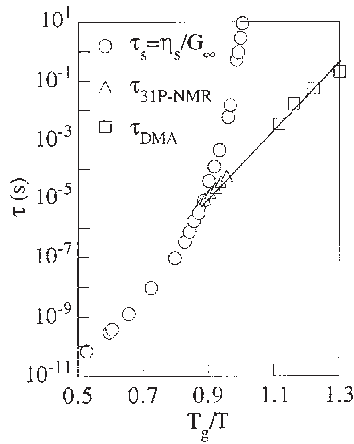


Fig. 3. Temperature dependence of the structural relaxation timescale  $\tau_s$  ( $\circ$  from [4,5,6]) calculated with the Maxwell relation and relaxation times obtained by  $^{31}\text{P}$  NMR ( $\Delta$  [3]) and DMA ( $\square$  [9]) probing the same secondary  $\beta_{\text{slow}}$ -process.

#### High frequency dynamics

Neutron scattering experiments have been carried out on the time-of-flight spectrometer MIBEMOL at the LLB (Saclay, France) with a closed hollow niobium cell in the temperature range 300-773 K. The incident wavelength was set to 6.2 Å, allowing scattering vectors up to  $q=1.9 \text{ Å}^{-1}$  at zero energy transfer. The full width at half height of the energy resolution was about 84  $\mu\text{eV}$  with a very clean triangular shape without wings. In  $\text{Na}_{0.5}\text{Li}_{0.5}\text{PO}_3$ , scattering is mainly coherent and furthermore, 87% of the signal is due to the  $\text{PO}_4$  tetrahedra. After usual corrections (detector efficiencies, sample container and instrumental background), the TOF spectra were converted in  $S(q, \omega)$ . Because of the high sample transmission (90%), multiple scattering corrections were not necessary.

If the  $\beta_{\text{fast}}$  process and the Boson peak are correlated, factorization of the dynamic susceptibility ( $\chi''(q, \omega) = S(q, \omega) / n(\omega)$ ) in  $q$  and  $\omega$  functions should be correct for the entire spectrum except at low frequencies where the  $q$ -dependent structural relaxation appears,

$$\chi''(q, \omega) = \chi''(\omega) \cdot S^{\text{inel}}(q) \quad (2)$$

It has been found that the data between  $1.0 \leq q \leq 5.0 \text{ Å}^{-1}$  are shown to overlap within experimental accuracy as well in the  $\beta_{\text{fast}}$  relaxation region as for the Boson peak. Furthermore, the shape of the inelastic structure factor  $S^{\text{inel}}(q)$  is not temperature dependent, i.e. whatever the relative weight of the  $\beta_{\text{fast}}$  relaxation with respect to the Boson peak.

Following an approach to the description of the low frequency Raman spectra in glasses proposed by Gochiyaev [10], these  $q$ -rescaled neutron spectra ( $S(\omega) = S(q, \omega) / S^{\text{inel}}(q)$ ) have been analysed with this model. In this approach, it is assumed that the Boson peak and the quasielastic scattering are due to a broad distribution of vibrational modes coupled with a coupling strength parameter  $\delta$  to a localized relaxation process defined by its relaxation time  $\tau$ . The distribution is given by the low temperature spectra without any relaxation where  $\delta \ll \omega_{\text{BP}}$  is the frequency of

the maximum of the Boson peak). In this phosphate glass, the shape of the Boson peak in neutron scattering is well described by the following phenomenological expression which contains only one unknown temperature dependent parameter: the frequency of the maximum of the Boson peak  $\omega_{bp}(T)$ :

$$S_{vib}(\omega, T) = \frac{n(\omega, T) \omega^3}{(\omega_{bp}^2(T) + \omega^2)^2} \quad (3)$$

On increasing temperatures,  $\delta$  increases towards  $\omega_{bp}$  leading to an overdamping and an instability of the Boson peak. In Fig. 4 are plotted some spectra together with this model showing a good agreement at all temperatures in the whole frequency range. The insert presents the temperature dependence of the renormalized frequency of the Boson peak maximum,  $\omega_{bp}^2 - \delta^2$ , leading to a crossover temperature  $T^* > T_g$  as already found in some glass-forming materials but from low frequency Raman spectra [11]. For these systems previously analysed within the MCT framework,  $T^*$  was found to be close to  $T_c$ .

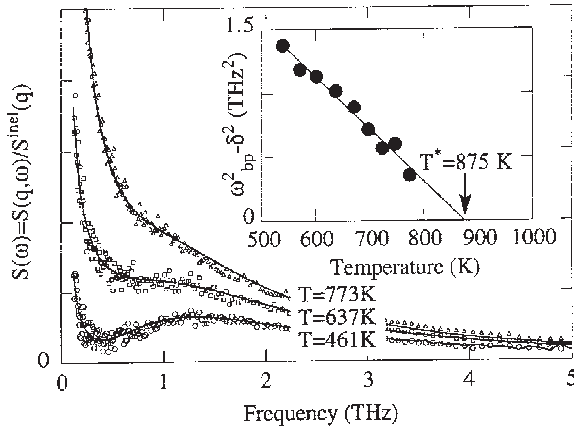


Fig. 4. Coherent neutron scattering spectra at three different temperatures for  $\text{Na}_{0.5}\text{Li}_{0.5}\text{PO}_3$ . Solids lines are fits with the convolution model of Gochiyaev [10]. The insert shows the temperature dependence of the renormalized frequency of the Boson peak maximum leading to an unstable mode at  $T^*=875$  K.

So in this temperature region, it seems that there is a transition from a "liquid-like" or relaxational behavior to a "solid-like" or vibrational one. However, the temperature  $T^*$  found in this compound is higher than the melting temperature  $T_m=749$  K so in order to give more reliability to these results and to their eventual relation with the MCT, light scattering experiments were carried out on this glass former and first analysed within the same frame.

Low-frequency Raman spectra have been obtained between 90 K and 923 K with a triple grating spectrometer using a  $90^\circ$  scattering geometry. Fig. 5 shows the room temperature depolarized spectrum on a reduced intensity scale [12]

$$I_R(\omega) = I(\omega) / (\omega(n(\omega) + 1)) = C(\omega)g(\omega) / \omega^2 \quad (4)$$

with its two contributions and as the neutron spectrum also on a reduced intensity scale

$$S_R(\omega) = S(\omega) / (\omega \cdot n(\omega)) = g(\omega) / \omega^2 \quad (5)$$

at the same temperature. In these two expressions,  $g(\omega)$  is the vibrational density of states while  $C(\omega)$  is the unknown light to excitation coupling function. It shows clearly that the shape of the Boson peak is almost independent of the scattering technique in this glass. In other words, the coupling coefficient  $C(\omega)$  appearing in the scattering formula for low frequency light scattering mechanism can only be weakly frequency dependent. This is confirmed by the frequency of the Boson peak maximum which is seen at nearly the same value in both spectra.

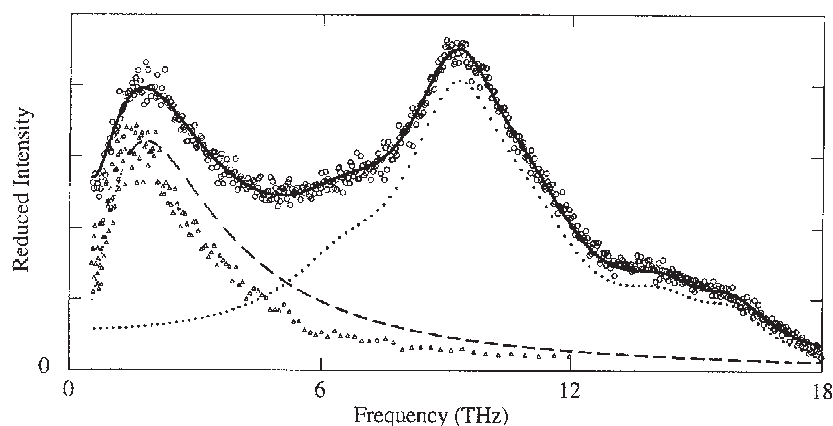


Fig. 5. ( $\circ$ , upper data) Low-frequency Raman spectrum in reduced intensity at 300 K. ( $\Delta$ , lower data) Neutron spectrum in reduced intensity at 300 K. The Raman spectrum is fitted (full line) by the superposition of two contributions: sum of optical modes (dotted line) and the Boson peak (dashed line) described by the same formula as in neutron scattering (3) except for a slightly higher frequency maximum of the Boson peak  $\omega_{bp}$ .

In summary, it has been verified first that the depolarization ratio was not frequency dependent in the low-frequency region around the Boson peak. Furthermore it has been found independent of temperature, i.e. whatever the relative weight of the  $\beta_{fast}$  relaxation with respect to the Boson peak. Again, this suggests a possible correlation between the quasielastic contribution and the inelastic one. Taking the same formula for the shape of the Boson peak (3) as in neutron scattering, these low-frequency Raman spectra have been fitted with this convolution model of Gochiyaev and while the temperature dependence of the frequency of the maximum of the Boson peak follows the same trend in both techniques, the coupling parameter  $\delta$  is notably stronger in light scattering results than in neutron ones, leading to a lower crossover temperature  $T^*$  (775 K) but still slightly above  $T_m$ . This larger contribution of the  $\beta_{fast}$  relaxation in light scattering spectra would require a very different coupling function  $C(\omega)$  for the scattering by relaxational excitations and vibrational ones in this glass-former. Moreover, these crossover temperatures pose the problem of the physical meaning of this temperature if it is the one where the glass falls out of equilibrium.

#### ACKNOWLEDGEMENTS

Authors are very grateful to Dr. E. Guéguen and Dr. R. Marchand from the "Verres et Céramiques" laboratory of Rennes I University for providing them with many excellent quality samples.

#### REFERENCES

1. W. Götze, in *Liquids Freezing and the glass transition*, edited by D. Levesque, J.P. Hansen and J. Zinn-Justin (Elsevier, New-York, 1991), p 287.
2. C.A. Angell and W. Sichina, *Ann. N.Y. Acad. Sci.*, **279**, 53 (1976).
3. B. Rufflé, S. Beaufils, J. Gallier, *Chem. Phys.*, **195**, 339 (1995).
4. R. Wäsche and R. Brückner, *Phys. Chem. Glasses*, **27**, 87 (1986).
5. R. Wäsche and R. Brückner, *Phys. Chem. Glasses*, **27**, 80 (1986).
6. B. Rufflé, unpublished viscosity data.
7. R. Böhmer, K.L. Ngai, C.A. Angell and D.J. Plazek, *J. Chem. Phys.*, **99**, 4201 (1993).
8. E. Rössler and P. Eierman, *J. Chem. Phys.*, **100**, 5237 (1994).
9. P.F. Green, D. Sidebottom and R.K. Brow, *J. Non-Cryst. Solids*, **172-174**, 1353 (1994).
10. V.Z. Gochiyaev, V.K. Malinovskiy, V.N. Navikov and A.P. Sokolov, *Philos. Mag. B*, **63**, 777 (1991).
11. A.P. Sokolov, A. Kisliuk, D. Quitmann, A. Kudlik, E. Rössler, *J. Non-Cryst. Solids*, **172-174**, 138 (1994).
12. R. Shuker and R. Gammon, *Phys. Rev. Lett.*, **25**, 222 (1970).

# Première partie

①

1.1  $\vec{P} = m_1 \vec{v}_1 + m_2 \vec{v}_2 = m_1 v_1 \vec{e}$  ,  $e_c = \frac{1}{2} m_1 v_1^2 + \frac{1}{2} m_2 v_2^2 = \frac{1}{2} m_1 v_1^2$

1.2  $[\vec{P} = \vec{P}'] \rightarrow m_1 v_1 \vec{e} = m_1 \vec{v}'_1 + m_2 \vec{v}'_2$  (1) eq. vectorielle

en  $\vec{x}$ )  $m_1 v_1 = m_1 v'_1 \cos \phi'_1 + m_2 v'_2 \cos \phi'_2$  (2)

en  $\vec{y}$ )  $0 = -m_1 v'_1 \sin \phi'_1 + m_2 v'_2 \sin \phi'_2$  (3)

$[e_c = e'_c] \rightarrow \frac{1}{2} m_1 v_1^2 = \frac{1}{2} m_1 v'^2_1 + \frac{1}{2} m_2 v'^2_2$  (4)

1.3 Dans ce système il y a quatre inconnues :  $v'_1, v'_2, \phi'_1, \phi'_2$ .  
( $v_1, m_1$  et  $m_2$  sont données) et seulement 3 équations donc il y a un nombre infini de solutions possibles. Pour le résoudre il faut une information supplémentaire. Par exemple connaître  $\phi'_1$ .

1.4 Par définition  $\vec{v}_{CG} = \frac{m_1 \vec{v}_1 + m_2 \vec{v}_2}{m_1 + m_2} \rightarrow \vec{v}_{CG} = \frac{m_1 v_1 \vec{e}}{m_1 + m_2}$

Ou voit que  $\vec{v}_{CG} = \vec{v}'_{CG}$  (par (1)). C'est normal car il n'y a pas de forces externes.

1.5  $\vec{v}'_1 = \vec{v}_1 - \vec{v}_{CG} = v_1 \vec{e} - \frac{m_1 v_1 \vec{e}}{m_1 + m_2} = \frac{(m_1 + m_2) v_1 \vec{e} - m_1 v_1 \vec{e}}{m_1 + m_2} = \frac{m_2 v_1 \vec{e}}{m_1 + m_2}$

$\vec{v}'_2 = \vec{v}_2 - \vec{v}_{CG} = 0 - \frac{m_1 v_1 \vec{e}}{m_1 + m_2} = - \frac{m_1 v_1 \vec{e}}{m_1 + m_2}$

$\rightarrow \boxed{\vec{v}'_1 = - \frac{m_2}{m_1} \vec{v}'_2}$   $\frac{m_2}{m_1} > 0 \rightarrow \vec{v}'_1$  opposée à  $\vec{v}'_2$

Pour l'observateur placé en C la vitesse du CG est nulle comme il est équilibré on peut le voir de  $\vec{v}_{CG} = \vec{v}_{CG} - \vec{v}_{CG} = 0$